




Spatial manipulation of topological defects in nematic shells

Luka Mesarec^{1,a} , Aleš Iglič¹, and Samo Kralj^{2,3}

¹ Laboratory of Physics, Faculty of Electrical Engineering, University of Ljubljana, Ljubljana, Slovenia

² Department of Physics, Faculty of Natural Sciences and Mathematics, University of Maribor, Maribor, Slovenia

³ Condensed Matter Physics Department, Jožef Stefan Institute, Ljubljana, Slovenia

Received 20 May 2022 / Accepted 28 June 2022 / Published online 25 July 2022

© The Author(s), under exclusive licence to EDP Sciences, SIF and Springer-Verlag GmbH Germany, part of Springer Nature 2022

Abstract It is well known that positions of topological defects (TDs) in liquid crystals can be manipulated experimentally by locally distorting the liquid crystalline (LC) order, as for example by melting induced by optical tweezers. In this work, we study numerically the nematic ordering profiles and the corresponding topological defect configurations in thin nematic liquid crystalline shells controlled by imposed local distortion of LC order. We demonstrate that within curved LC films such manipulations could be strongly affected by local Gaussian curvature if it exhibits strong spatial variations. We use mesoscopic approach in which the shell geometry and LC orientational order are described by curvature of the surface and nematic order parameter tensor. For illustration purposes, we consider LC shells exhibiting spherical topology. We show that on increasing prolateness of shells, which imposes spatially inhomogeneous Gaussian curvature, TDs are relatively strongly “glued” to a local Gaussian curvature.

1 Introduction

Topological defects (TDs) correspond to localized deformations in a physical field that are topologically protected [1]. Due to its topological origin, this research field is strongly interdisciplinary [2]. Consequently, it is of interest to all branches of physics. The essential property of TDs is their topological charge [1, 3], which is a conserved quantity. Therefore, conservation rules govern transformations among different defects arrangements, such as merging of defects and splitting [4, 5]

An ideal testing ground to study the impact of topology and geometry on TDs are nematic liquid crystalline (LC) shells [6–10]. They consist of thin nematic films, roughly of typical molecular length thickness, covering micrometers-sized colloidal objects. Nowadays, one can prepare colloids of almost arbitrary topology experimentally [11]. TDs within films could be visualized using relatively simple methods, such as polarizing microscopy [12]. Furthermore, nematic LCs [12] are extremely stimuli-responsive owing to their inherent softness. Finally, nematic shells are promising building blocks to form different new effective materials in near future, e.g., as colloidal crystals [6].

The simplest nematic LCs [12] consist of anisotropic (e.g., rod-like) LC molecules. They exhibit liquid-like

properties combined with orientational order. The latter is at the mesoscopic level commonly described by the nematic director field \vec{n} , pointing along a local average molecular direction. In bulk equilibrium, \vec{n} is spatially homogeneously aligned along a single symmetry breaking direction. Nematic shells exhibit effectively two-dimensional (2D) systems, where orientations of \vec{n} are confined within a 2D curved film [6]. Consequently, such structures are in general dominated by TDs.

In 2D nematic films, point topological defects are characterized by the winding number m , which can be half integer due to $\pm\vec{n}$ invariance. It describes the number of rotations of \vec{n} on encircling by any path the defect center counter clockwise. TDs characterized by a positive and negative value of m are referred to as *defects* and *antidefects*, respectively. The free energy costs of a single TD in a flat geometry are proportional to m^2 . Consequently, if a TDs bearing a relatively high topological charge is enforced, it tends to decompose into elementary charges bearing $|m| = 1/2$. Within a closed surface, the total charge in the system is determined [13, 14] by the Gauss–Bonnet and Poincaré–Hopf theorems: $\frac{1}{2\pi} \oint K d^2r = 2(1 - g) = m_{tot}$. Here K stands for the Gaussian curvature, $dA = d^2r$ is the surface element of a closed 2D manifold, g is the genus of the surface (i.e., number of holes), and m_{tot} stands for the total topological charge within the system. For the spherical topology ($g = 0$) it holds $m_{tot} = 2$. Therefore, a large enough spherical film hosts four TDs [7, 15] bearing $m = 1/2$. Furthermore, regions exhibiting

Guest editors: Fabrizio Croccolo, Aleksandra Drozd-Rzoska, Samo Kralj, Szymon Starzonek.

^a e-mail: luka.mesarec@fe.uni-lj.si (corresponding author)

$K > 0$ ($K < 0$) attract [16–19] TDs bearing $m > 0$ ($m < 0$). Therefore, a surface patch ΔA bearing positive (negative) Gaussian curvature acts locally as a “smeared” negative (positive) topological charge given by $\Delta m_K = -\frac{1}{2\pi} \iint K dA$. Consequence of this tendency is the Effective Topological Charge Cancellation (ETCC) mechanism [20] which claims that each surface patch ΔA , characterized by the spatially averaged Gaussian curvature $\bar{K} = \frac{1}{\Delta A} \iint K dA$, tends to be topologically neutral, i.e. $\Delta m_{eff} = \Delta m_K + \Delta m = 0$. Here Δm stands for the total charge of TDs and Δm_{eff} stands for the effective charge within the surface patch. Armed by Gauss–Bonnet & Poincaré–Hopf theorems along with the ETCC mechanism one could efficiently predict the number of TDs within a system.

One of the key LC features is softness, i.e., strong responsiveness to local stimuli. In particular, it has been shown that one could efficiently manipulate nematic TDs using laser beams [21–24]. Namely, a laser beam locally melts orientational order. Similar LC configuration is formed within the core of topological defects. Therefore, it is advantageous for TDs to be assembled within regions with reduced nematic order because the condensation melting penalty to form the defect core is reduced. Due to similar phenomenon, TDs in arbitrary physical field tend to be pinned to “impurities”. However, we show in this contribution that in effectively 2D curved manifolds, nematic TDs are relatively strongly “glued” to a local Gaussian curvature.

The plan of the paper is as follows. In Sect. 2 we introduce the model. The results are presented in Sect. 3 and conclusions are summarized in Sect. 4.

2 Model

To describe the shapes of 2D curved manifolds and the nematic ordering within them, we use mesoscopic modeling, where the properties of the system are described using the curvature tensor \underline{C} and the nematic order tensor \underline{Q} . The Weingarten curvature tensor \underline{C} [10] determines the local surface curvature:

$$\underline{C} = C_1 \vec{e}_1 \otimes \vec{e}_1 + C_2 \vec{e}_2 \otimes \vec{e}_2, \quad (1)$$

where the unit vectors $\{\vec{e}_1, \vec{e}_2\}$ point along the surface principal directions exhibiting principal curvatures $\{C_1, C_2\}$. In this formulation, the local mean curvature (H) and the Gaussian curvature (K) are the invariants of \underline{C} and can be calculated as:

$$H := \frac{Tr[\underline{C}]}{2} = \frac{C_1 + C_2}{2}, \quad K := Det[\underline{C}] = C_1 C_2 \quad (2)$$

Local nematic orientational order on the surface is described in terms of the 2D tensor order parameter \underline{Q} . The molecules exhibiting orientational ordering are bound to lie in the local tangent plane of the surface

and are otherwise unconstrained. We assume rod-like shaped molecules with the so-called head-to-tail invariance. Tensor \underline{Q} can be expressed in the diagonal form as [15]

$$\underline{Q} = \lambda(\vec{n} \otimes \vec{n} - \vec{n}_\perp \otimes \vec{n}_\perp), \quad (3)$$

where the unit vectors \vec{n} and \vec{n}_\perp are its eigenvectors, while $\lambda \in [0, 1/2]$ and $-\lambda$ are the corresponding eigenvalues. The lower bound $\lambda_{\min} = 0$ corresponds to locally isotropic state with no orientational order, while the upper bound $\lambda_{\max} = 1/2$ corresponds to locally ordered state with molecules rigidly aligned along the direction \vec{n} , commonly referred to as the nematic director field.

We express the total free energy functional of the LC shell surface as $F = \iint f d^2r$, where the free energy density $f = f_c + f_e$ consists of the order condensation (f_c) and elastic (f_e) term. We use a minimal model to illustrate the features of our interest. For this purpose, we express the nematic elasticity in terms of a single elastic constant k . The energy densities are expressed as [15, 20]

$$f_c = -\alpha Tr \underline{Q}^2 + \beta (Tr \underline{Q}^2)^2, \quad (4a)$$

$$f_e = k Tr \left((\nabla_s \underline{Q})^2 \right). \quad (4b)$$

The orientational ordering exists for positive values of material constants α and β . The material dependent order parameter correlation length is defined as $\xi = \sqrt{k/|\alpha|}$ and estimates the distance at which a local perturbation in order parameter relaxes on a flat surface. The quantity R is introduced as a characteristic geometrically imposed length in the system and is defined as the radius of the sphere with the same surface area as the surface of the investigated shell. The bulk equilibrium value of order parameter in flat geometries is given by $\lambda_0 = \sqrt{\alpha/\beta}/2$.

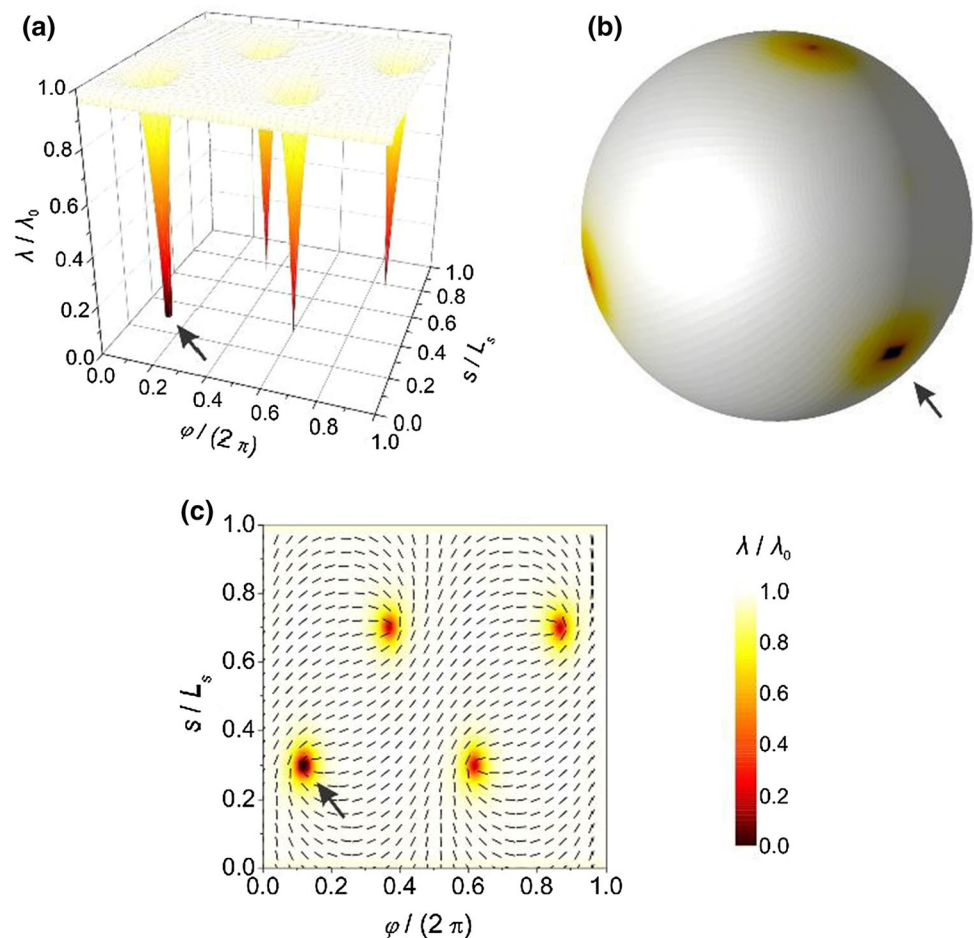
LC shells in this study are restricted to axially symmetric surfaces of revolution with rotational symmetry about the z -axis. The position vector \vec{r} of a generic point lying on such surface can be parametrized as

$$\vec{r}(\varphi, s) = \rho(s) \cos \varphi \vec{e}_x + \rho(s) \sin \varphi \vec{e}_y + z(s) \vec{e}_z, \quad (5)$$

where $\rho(s)$ and $z(s)$ are the coordinates of the LC shell profile in the (ρ, z) -plane, $\varphi \in [0, 2\pi]$ stands for the azimuthal angle and s represents the arc length of the profile curve [20, 25–27]. The unit vectors $\{\vec{e}_x, \vec{e}_y, \vec{e}_z\}$ determine the Cartesian coordinate system. On the surface of revolution, parallels and meridians represent the lines of principal curvature. We set that the principal directions (see Eq. 1) $\{\vec{e}_1, \vec{e}_2\}$ point along meridians ($\varphi = \text{const.}$) and parallels ($s = \text{const.}$), respectively.

In this paper we considered fixed axisymmetric surfaces, defined by their profile curve, on which the nematic ordering was calculated by minimizing the free energy with respect to \underline{Q} . In simulations, shell surface is

Fig. 1 Equilibrium nematic ordering profile on a spherical shell, where the point affected by the laser beam (*distortion*) is denoted by an arrow in each panel. **a** The nematic order parameter λ variation in the (φ, s) plane. **b** The shell's shape with the superimposed color code determined nematic order parameter. **c** Superimposed nematic director field and order parameter profile λ in the (φ, s) plane. The calculations were performed for $R/\xi = 10$



represented by 100×100 points. Equilibrium textures are calculated with the Monte Carlo method, i.e. by randomly changing the tensor \underline{Q} in each of these points until the total free energy cannot be further minimized. Laser beam was modeled by imposing a boundary condition of locally melted orientational order. Melting is enforced by setting $\lambda = 0$ in some points, while the orientational ordering is calculated by minimizing the total free energy in all other points. Smooth transition from the melted region to the surrounding ordered regions is enforced by Eq. (4b) since any sharp changes result in energy penalty.

3 Results

Of our interest is manipulation of TDs in nematic shells by laser (or some other means) driven local distortions, which give rise to local melting of nematic order. In simulations we simulate such distortions via a melted region whose spatial position within prolate shells is varied. It is well known that local melting attracts TDs [21–24] deep in the nematic phase. Namely, both melting and TDs introduce a relatively strong condensation penalty. Since the core of a TD is essentially melted, the total free energy penalty is in general reduced if the

melted region and TD occupy the same region. Henceforth we refer to a melted region as *distortion*.

For the reference we plot in Fig. 1 the configuration of TDs in a spherical nematic shell, where the *distortion* is marked by an arrow. In this case the Gaussian curvature is spatially constant and consequently the relative position of TDs is determined by their mutual elastic repulsion and in our case also by the location of the *distortion*. More detailed analytical and numerical studies are given in Refs.[7, 8, 15]. Four $m = 1/2$ TDs occupy the vertices of a tetrahedron inscribed within the sphere {see Fig. 1b and c). At the core of defects, whose linear size is roughly given by the nematic order parameter correlation length, the nematic order is melted (Fig. 1a). We henceforth refer to such a spatial distribution of TDs as the *tetrahedron* configuration. We can place the *distortion* on any point on the spherical surface and the closest defect will get trapped within its center. Because of mutual repulsion, other defects rearrange in such a way that the *tetrahedron* configuration symmetry is conserved. Note that the linear size of the *distortion* has to be comparable to the nematic correlation length ξ in order to effectively trap TDs. If the distorted region represents only 1 point in our 100×100 surface discretization, it doesn't significantly change the orientational ordering profile. Therefore, in

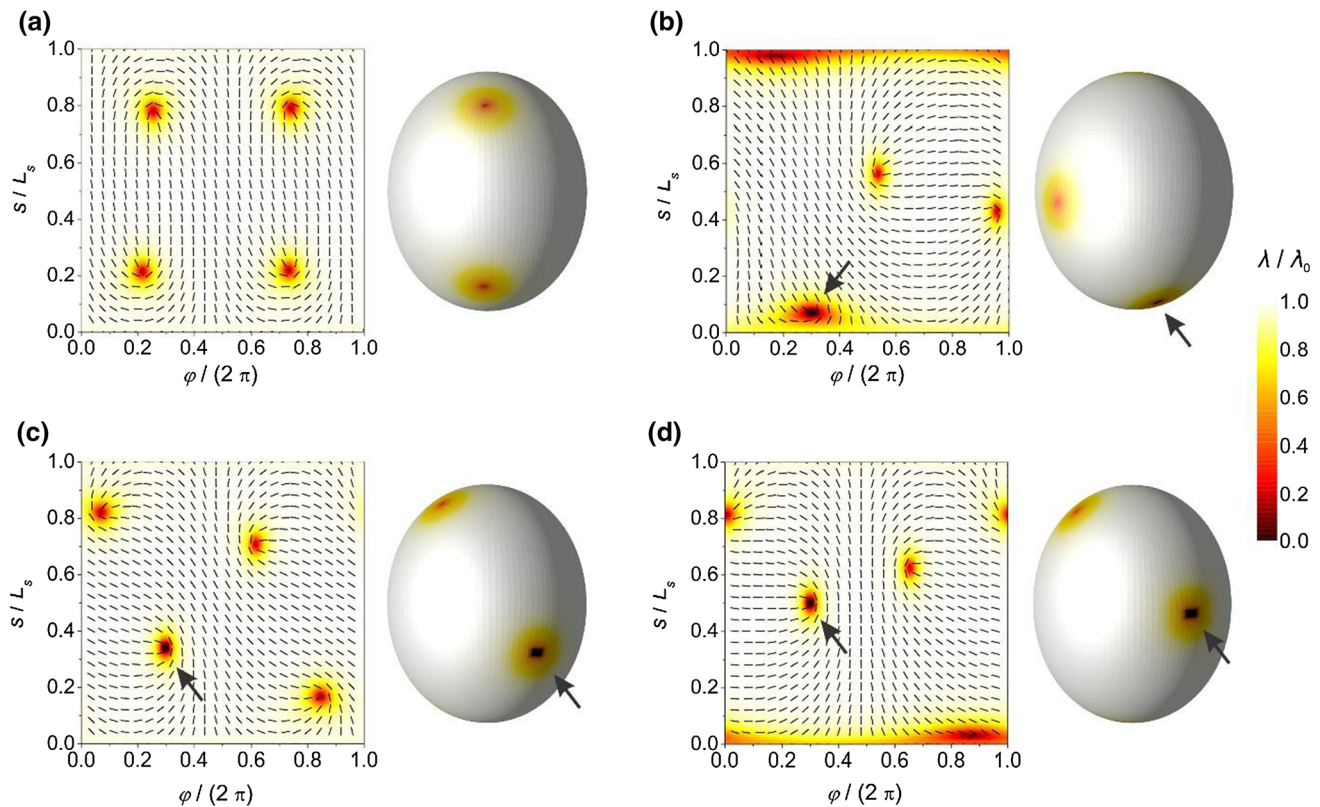


Fig. 2 Equilibrium nematic ordering profiles on a weakly prolate shell. Panel **a** represents the case without the *distortion* (laser beam), while different positions of the *distortion* are denoted by arrows in the panels (**b**, **c**, **d**). Left-hand side in each panel shows the superimposed nematic director

field and color code determined order parameter profile λ in the (φ, s) plane, while the shell shapes with the superimposed nematic order parameter are presented in the right-hand side in each panel. The calculations were performed for $R/\xi = 10$

our simulations, the *distortion* is represented by 3×3 points.

Firstly, we consider weakly prolate shells that are close to a sphere. TDs are attracted to regions exhibiting maximal Gaussian curvature. Consequently, pairs of TDs in the upper and lower region of an ellipsoid are shifted toward the corresponding poles as shown in Fig. 2a. Next, we introduce a *distortion* whose position we vary. In Fig. 2b we show the case where the *distortion* is slightly above the lower pole. One sees that the closest TD moves toward this point and becomes trapped within it. Due to the mutual elastic interaction among TDs, all the remaining TDs rearrange in order to minimize their mutual repulsion. Similar phenomenon is observed in Fig. 2c, d. Figure 2 illustrates that in such a geometry one can efficiently manipulate the position of TDs. Due to spatially dependent Gaussian curvature their relative position in general significantly departs from the reference *tetrahedron* configuration. The spatial profile K for weakly prolate shells presented in Fig. 2 is shown in Fig. 3 (dashed line).

Next, we consider relatively pronounced prolate shells where the Gaussian curvature exhibits strong spatial dependency (Fig. 3, full line). In this case, TDs are relatively strongly “glued” to the regions close to the

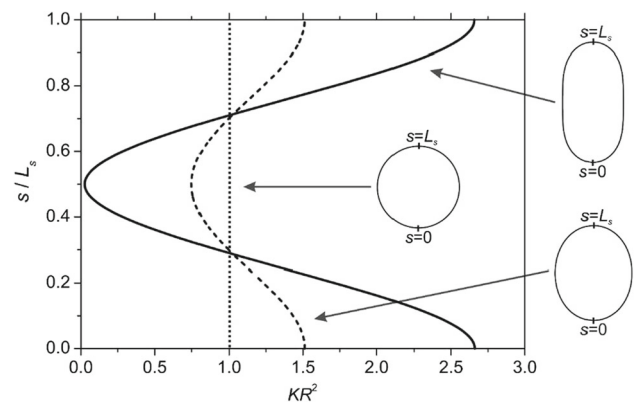


Fig. 3 Gaussian curvature $K(s)$ spatial variations for three different shapes (sphere, weakly prolate shape, strongly prolate shape) analyzed in this paper. L_s is the length of the profile curve and R the radius of the sphere with the same surface area as the surface of the investigated shape

poles. In Fig. 4a we show the configuration of TDs in the absence of a *distortion*: the defects are placed relatively close to the poles. In Fig. 4b we introduce a *distortion* close to the lower pole. One sees that one

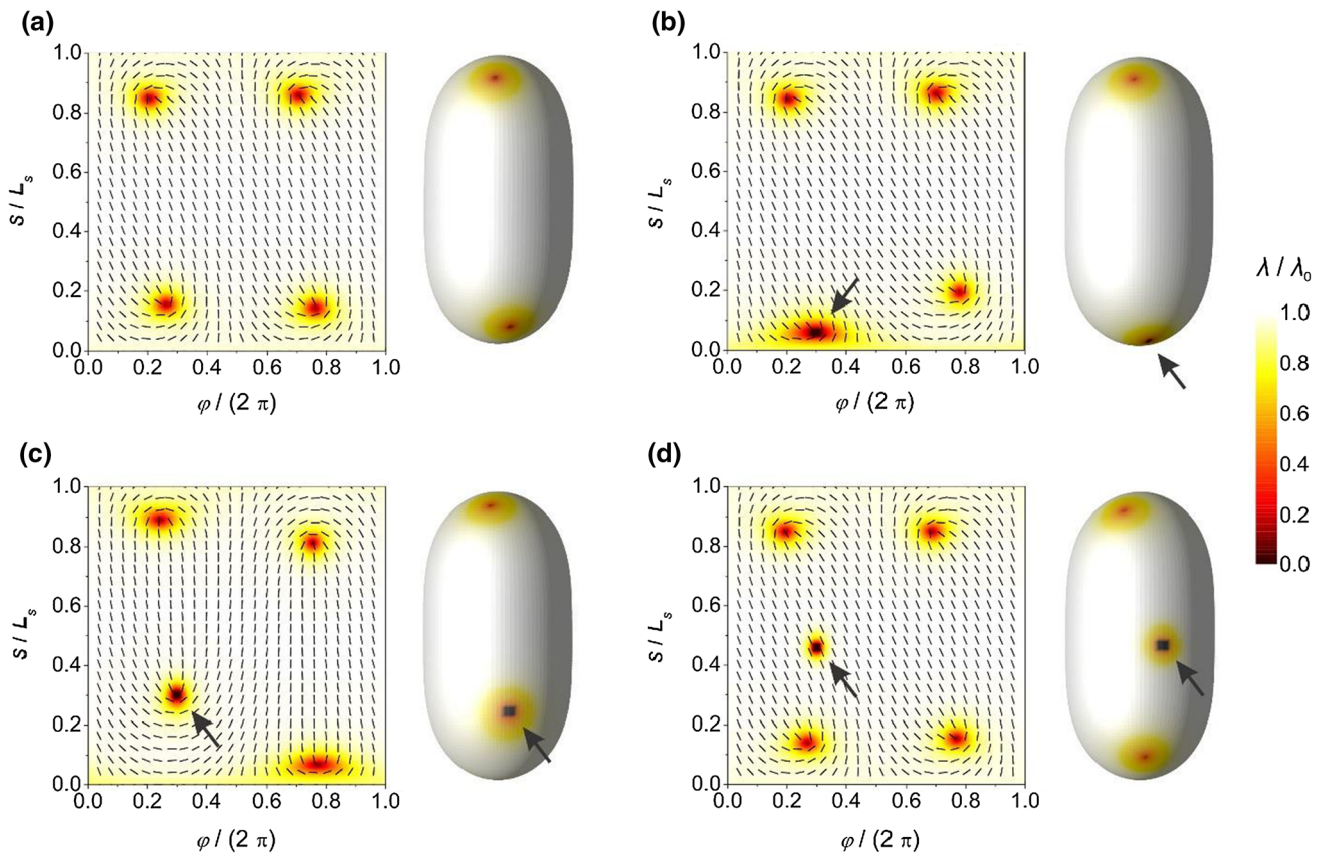


Fig. 4 Equilibrium nematic ordering profiles on a strongly prolate shell. Panel **a** represents the case without the laser beam (*distortion*), while different positions of the *distortion* are denoted by arrows in the panels (**b**, **c**, **d**). Left-hand side in each panel shows the superimposed nematic director

field and color code determined order parameter profile λ in the (φ, s) plane, while the shell shapes with the superimposed nematic order parameter are presented in the right-hand side in each panel. The calculations were performed for $R/\xi = 10$

can manipulate the relative position of the two TDs which are adjacent to this pole. Note that in the region close to the poles Gaussian curvature exhibits a relatively large value. One TD is always trapped within the *distortion*, while the other adopts the position that reflects the interplay between the mutual interaction of these defects and their interaction with the local Gaussian curvature. The position of other two TDs remains essentially the same. This reveals that their position is dominantly influenced by the local Gaussian curvature and their mutual elastic repulsion. If the *distortion* is dragged outside of the region where K is relatively large, the trapped defect depins from the *distortion* and the defect configuration favored by K is recovered (Fig. 4d).

4 Conclusions

Of our interest was manipulation of TDs within nematic shells exhibiting spherical topology. In our simulations we inserted a localized melted region (to which we

refer as a *distortion*) and observed its impact on spatial distribution of TDs. Experimentally, this could be achieved, e.g., by using a narrow laser beam. In this case, in addition to thermal effects, also electromagnetic field might play the role. In our approach we neglect the latter effect. Our simulations reveal that responses to *distortions* strongly depend on geometrical details, i.e., spatial dependence of the Gaussian curvature. In cases where the Gaussian curvature is constant, the closest TD gets trapped within the *distortion*, while the remaining TDs redistribute and adopt the configuration which minimizes their mutual elastic repulsion. The relative positions of TDs are enslaved by the *distortion*, however, the symmetry of their arranging is conserved. In the case where K exhibits a weak spatial dependence, we observe qualitative changes in the distribution of TDs as a function of the *distortion* position. In this case the assembly of TDs is sensitively dependent on the interplay between the local melting penalty due to the *distortion*, repulsion interaction among all TDs, and their attraction to the Gaussian curvature. Even stronger qualitative changes are observed in cases

where K exhibits a relatively strong spatial dependence. In this case, the distortion can strongly affect two defects near a pole if it is located close to the TDs. The two TDs at the opposite pole are relatively weakly affected, which means that strongly spatially dependent K profile decouples the pairs of TDs at opposite poles. Furthermore, TDs are in such cases relatively strongly “glued” within regions exhibiting relatively large values of K . One could drag a TD if it is initially trapped within the distortion within an area where K does not significantly change. However, if it is dragged toward the region exhibiting sufficiently lower value of K , the defect depins from the distortion and restores the configuration favored by spatial K dependence.

Ability to positionally manipulate TDs opens opportunities to diverse applications. For instance, TDs in LCs could efficiently trap appropriate nanoparticles (NPs) within their cores [28, 29]. Such NPs should either be appropriately surface decorated or should be small enough. These conditions are embodied in the requirement [12] $R/d_e < 1$, where R stands for the characteristic NP linear size and d_e stands for the surface extrapolation length. The latter is inversely proportional with the LC-NP surface anchoring interaction strength. Thus via positional manipulation of TDs one could indirectly control arrangements of trapped NPs which might be exploited in diverse nanotechnological applications. For example, nematic shells immersed in an appropriate fluid could potentially form micron-sized crystal structures [6], where the “valence” of basic constituents (i.e., nematic shells) is determined by TDs within the shell. In such structures, positional manipulation of TDs would affect local bonding conditions. Furthermore, TDs are sources or relatively long-ranged distortions in nematic order. Moving their cores in general causes apparent local optical changes which might be exploited in diverse optical devices.

Acknowledgements The authors acknowledge the support of a Slovenian Research Agency (ARRS) grants P1-0099, P2-0232, J1-2457 and J3-3066. The paper is associated with the International Seminar on Soft Matter & Food – Physico-Chemical Models & Socio-Economic Parallels, 1st Polish-Slovenian Edition, Celestynów, Poland, 22–23 Nov., 2021; directors: Dr. hab. Aleksandra Drozd-Rzoska (Institute of High Pressure Physics PAS, Warsaw, Poland) and Prof. Samo Kralj (Univ. Maribor, Maribor, Slovenia).

Author contribution statement

SK initiated this study and developed the theoretical model. LM developed a Monte Carlo program for the calculation of nematic profiles and performed the numerical simulations. SK, AI and LM wrote the manuscript.

Data availability The datasets generated during and/or analyzed during the current study are available from the corresponding author on reasonable request.

References

1. N.D. Mermin, The topological theory of defects in ordered media. *Rev. Mod. Phys.* **51**(3), 591 (1979)
2. W.H. Zurek, Cosmological experiments in superfluid helium? *Nature* **317**(6037), 505–508 (1985)
3. G.E. Volovik, O.D. Lavrentovich, Topological dynamics of defects: boojums in nematic drops. *Zh. Eksp. Teor. Fiz.* **85**(6), 1997–2010 (1983)
4. D. Svenešek, S. Žumer, Instability modes of high-strength disclinations in nematics. *Phys. Rev. E* **70**(6), 061707 (2004)
5. S. Kralj, B.S. Murray, C. Rosenblatt, Decomposition of strongly charged topological defects. *Phys. Rev. E* **95**(4), 042702 (2017)
6. D.R. Nelson, Toward a tetravalent chemistry of colloids. *Nano Lett.* **2**(10), 1125–1129 (2002)
7. V. Vitelli, D.R. Nelson, Nematic textures in spherical shells. *Phys. Rev. E* **74**(2), 021711 (2006)
8. G. Skačej, C. Zannoni, Controlling surface defect valence in colloids. *Phys. Rev. Lett.* **100**(19), 197802 (2008)
9. T. Lopez-Leon, V. Koning, K.B.S. Devaiah, V. Vitelli, A. Fernandez-Nieves, Frustrated nematic order in spherical geometries. *Nat. Phys.* **7**(5), 391–394 (2011)
10. R. Rosso, E.G. Virga, S. Kralj, Parallel transport and defects on nematic shells. *Contin. Mech. Thermodyn.* **24**(4), 643–664 (2012)
11. B. Senyuk, Q. Liu, S. He, R.D. Kamien, R.B. Kusner, T.C. Lubensky, I.I. Smalyukh, Topological colloids. *Nature* **493**(7431), 200–205 (2013)
12. M. Kleman, O.D. Lavrentovich (eds.), *Soft Matter Physics: An Introduction* (Springer, New York, NY, 2003)
13. H. Poincaré, Sur les courbes définies par les équations différentielles. *J. Math. Pures. Appl.* **4**(2), 151–217 (1886)
14. R.D. Kamien, The geometry of soft materials: a primer. *Rev. Mod. Phys.* **74**(4), 953 (2002)
15. S. Kralj, R. Rosso, E.G. Virga, Curvature control of valence on nematic shells. *Soft Matter* **7**(2), 670–683 (2011)
16. V. Vitelli, A.M. Turner, Anomalous coupling between topological defects and curvature. *Phys. Rev. Lett.* **93**(21), 215301 (2004)
17. M. Bowick, D.R. Nelson, A. Travasset, Curvature-induced defect unbinding in toroidal geometries. *Phys. Rev. E* **69**(4), 041102 (2004)
18. M.A. Bates, G. Skačej, C. Zannoni, Defects and ordering in nematic coatings on uniaxial and biaxial colloids. *Soft Matter* **6**(3), 655–663 (2010)
19. L.V. Mirantsev, E.J.L. de Oliveira, I.N. de Oliveira, M.L. Lyra, Defect structures in nematic liquid crystal shells of different shapes. *Liq. Cryst. Rev.* **4**(1), 35–58 (2016)
20. L. Mesarec, W. Gózdź, A. Iglič, S. Kralj, Effective topological charge cancellation mechanism. *Sci. Rep.* **6**(1), 1–12 (2016)
21. A. Nych, J.I. Fukuda, U. Ognysta, S. Žumer, I. Muševič, Spontaneous formation and dynamics of half-skyrmions in a chiral liquid-crystal film. *Nat. Phys.* **13**(12), 1215–1220 (2017)

22. U. Tkalec, M. Ravnik, S. Čopar, S. Žumer, I. Mušević, Reconfigurable knots and links in chiral nematic colloids. *Science* **333**(6038), 62–65 (2011)
23. Q. Liu, B. Senyuk, M. Tasinkevych, I.I. Smalyukh, Nematic liquid crystal boojums with handles on colloidal handlebodies. *Proc. Natl. Acad. Sci.* **110**(23), 9231–9236 (2013)
24. I.I. Smalyukh, Knots and other new topological effects in liquid crystals and colloids. *Rep. Prog. Phys.* **83**(10), 106601 (2020)
25. W.T. Gózdź, Spontaneous curvature induced shape transformations of tubular polymersomes. *Langmuir* **20**(18), 7385–7391 (2004)
26. W.T. Gózdź, Influence of spontaneous curvature and microtubules on the conformations of lipid vesicles. *J. Phys. Chem. B* **109**(44), 21145–21149 (2005)
27. W.T. Gózdź, The interface width of separated two-component lipid membranes. *J. Phys. Chem. B* **110**(43), 21981–21986 (2006)
28. H. Kikuchi, M. Yokota, Y. Hisakado, H. Yang, T. Kajiyama, Polymer-stabilized liquid crystal blue phases. *Nat. Mater.* **1**(1), 64–68 (2002)
29. E. Karatairi, B. Rožič, Z. Kutnjak, V. Tzitzios, G. Nounesis, G. Cordoyiannis, J. Thoen, C. Glorieux, S. Kralj, Nanoparticle-induced widening of the temperature range of liquid-crystalline blue phases. *Phys. Rev. E* **81**(4), 041703 (2010)